ACS APPLIED POLYMER MATERIALS

Forum Article

Cite This: ACS Appl. Polym. Mater. 2020, 2, 1031−1042

pubs.acs.org/acsapm

Multiple Physical Bonds to Realize Highly Tough and Self-Adhesive Double-Network Hydrogels

Dong Zhang,[†,¶] Fengyu Yang,[†,¶] Jian He,[†] Lijian Xu,[*,†,∥] Ting Wang,[†,⊥] Zhang-Qi Feng,[†,#] Yung Chang,[▽] Xiong Gong,[‡] Ge Zhang,[§] and Jie Zheng[*,†]

[†]Department of Chemical and Biomolecular Engineering, [‡]Department of Polymer Engineering, and [§]Department of Biomedical Engineering, The University of Akron, Akron 44325, Ohio, United States

[∥]Hunan Key Laboratory of Biomedical Nanomaterials and Devices College of Life Sciences and Chemistry, Hunan University of Technology, Zhuzhou 412007, China

[⊥]State Key Laboratory of Bioelectronics, Southeast University, Nanjing 210096, China

[#]School of Chemical Engineering, Nanjing University of Science and Technology, Nanjing 210094, China

[▽]Department of Chemical Engineering R&D Center for Membrane Technology, Chung Yuan Christian University, Taoyuan 320, Taiwan

Supporting Information

ABSTRACT: Tough and adhesive hydrogels have shown great potential in wearable devices, flexible electronics, and human−machine interfaces. However, most existing tough hydrogels have weak surface adhesion, or highly adhesive hydrogels have low mechanical strength. It remains a long-standing challenge to develop the hydrogels with both highly mechanical and adhesive properties. Here, we design and fabricate a fully physical double network hydrogel of Agar/pHEAA-AAc-Fe^{3+}, which consisted of the first Agar network by hydrogen bonds and the second poly(*N*-hydroxyethyl acrylamide) (pHEAA)-AAc-Fe^{3+} network by multiple hydrogen and ionic bonds. Because of the special interpenetrating network structures and all reversible physical cross-linking effects, the resulting optimal hydrogels achieved high mechanical performances (breaking strength of 960 kPa, fracture strain of 11, tearing energy of 1306 J/m^3, and energy dissipation of 1644 kJ/m^3), high stiffness/toughness recovery of 75/51.9% at 80 °C after 30 min resting, and certain degrees of self-healing property. Meanwhile, Agar/pHEAA-AAc-Fe^{3+} hydrogels also exhibited strong surface adhesion to various untreated solid surfaces, with high interfacial toughness of 2619−4414 J/m^2. Both high bulk and interfacial toughness are mainly contributed to synergetic cooperation of multiple noncovalent interactions and double-network structure. This work introduces a set of design concept, hydrogel system, and synthesis approach that could be applicable to other polymers, elastomers, and soft materials to meet different demands (toughness, extensibility, healing, and adhesion) in different bench-to-bedside applications.

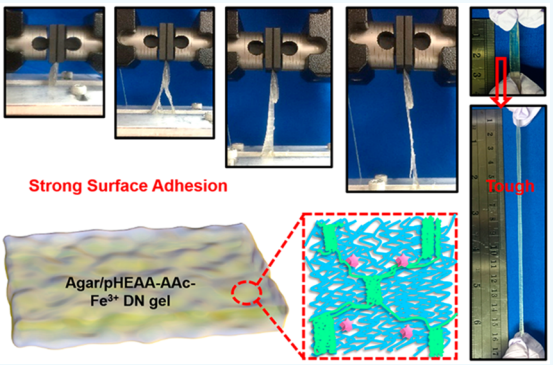

KEYWORDS: *double-network hydrogel, tough hydrogel, physical cross-linking, surface adhesion, self-healing*

INTRODUCTION

Polymeric hydrogels, as classical soft-and-wet materials, contain abundant water in three-dimensional (3D) polymer networks.[1−5] The abundance of water in hydrogels, on one hand, offers a unique combination of structural and functional properties (e.g., highly structural flexibility/adaptivity for stimuli-responsive actuations,[6,7] biomimetic resemblance to soft tissues,[8,9] and soft carriers and hosts for drugs and gene[10,11]); on the other hand, it also makes hydrogels not only mechanically weak in bulk but also adhere poorly to most surfaces. Great efforts and progress have been made to enhance the bulk mechanical properties of hydrogels by introducing new network structures, additives, cross-linkers, or their combinations to enhance network interactions and energy dissipation. These tough hydrogels include double network (DN) hydrogels,[12−14] nanocomposite (NC) hydrogels,[15−17] slide ring polymer hydrogels,[18,19] macromolecular microsphere composite (MMC) hydrogels,[20] tetra-ethylene glycol (PEG) hydrogels,[21,22] and others.[23−25] However, the challenge still remains; that is, when applying these tough hydrogels to different solid surfaces for some adhesive applications (e.g., wearable devices, electronic skins, 3D printing systems, human−machine interfaces), most hydrogels poorly adhere on the surfaces due

Special Issue: Toughening of Networks and Gel Through Molecular Design

Received: September 20, 2019
Accepted: November 19, 2019
Published: December 5, 2019

DOI: 10.1021/acsapm.9b00889
ACS Appl. Polym. Mater. 2020, 2, 1031−1042

to very weak surface adhesion (1−100 J/m^2).[26−29] This indicates that bulk toughness and surface adhesion in hydrogels stem from two different natures of intermolecular interactions; that is, the former one comes from polymer network interactions inside hydrogels, while the latter one originates from both network interactions and polymer−surface interactions. While high bulk toughness of hydrogels does not necessarily guarantee high interfacial toughness, high interfacial toughness requires high bulk toughness of hydrogels, because strong toughness allows hydrogels to be peeled from surfaces before fracture themselves.

Undoubtedly, adhesive hydrogels with both high bulk/interfacial toughness have attracted much attention to many existing and emerging applications. Current strategies for preparing tough hydrogel adhesives generally involve (i) the introduction of mussel-inspired adhesive groups,[30] (ii) the surface modification of the substrates,[31,32] (iii) the use of cytotoxic bonding agents/glues,[33] (iv) the special design of topological entanglement at interfaces,[34] and (v) the physical adhesion interactions. Mussel-inspired adhesive hydrogels often require oxidants to produce adhesive catechol or 3,4-dihydroxyphenylalanine (DOPA) groups for surface adhesion. However, these mussel-inspired hydrogels generally showed weak mechanical properties, poor deformability, and short-term adhesiveness. PAMPS/PAAm and PAAm/alginate DN hydrogels[31,32] have been well-recognized by their superior bulk toughness, and they have also been chemical anchorage on different solid surfaces (glass, ceramics, titanium silicon wafer, and aluminum) to achieve high interfacial toughness of ∼1000 J/m^2. However, a proverbial drawback of chemical anchorage is that once interfacial bonding is broken, surface adhesion will be largely destroyed, leading to single or limited reusability. Lack of reversible adhesive behaviors were also observed in cyanoacrylate-based adhesive hydrogels[33] and covalent topological adhesive hydrogels.[34,35] Differently, noncovalent adhesion made of hydrogen bonding, hydrophobic interaction, electrostatic interaction, host−guest interaction, and metal coordination can achieve instant, reversible, and on-demanding attachment and detachment, but such noncovalent adhesion usually has low adhesion energy (1−100 J/m^2). Until recently, several noncovalent adhesive hydrogels (e.g., Agar/pHEAA and Agar/pAAEE hydrogel) can instantly adhere on various nonporous solid substrates without any pretreatment but with high interfacial toughness of 1000−7000 J/m^2. Particularly, Agar/pAAEE hydrogel reversibly adhere on and peel off from the glass 100 times, while still retaining relatively strong/durable adhesion energy (250 J/m^2). Further inspection of these tough adhesive hydrogels highlights the importance of bulk toughness contributed by physically cross-linked DN networks, which help to not only dissipate energy upon debonding but also rapidly recover the adhesion after debonding and rejoining.

Considering the enormous diversity and combinations of noncovalent bonds (hydrogen bonds, hydrophobic interaction, $\pi-\pi$ stacking, host−guest interaction, ionic interaction, dipole−dipole interactions, and metal coordination), they can be used separately or in combination to construct different networks and dissipate energy by rupturing different types of noncovalent bonds. In addition, the reversible breaking/reforming of noncovalent bonds within polymer networks and between the networks and substrates could offer a higher possibility for the strong self-recovery and reversible adhesive properties of hydrogels. Among them, hydrogen bonds and ionic interactions, due to their simple and automatous nature, are the two common noncovalent bonds used for improving the mechanical properties of DN hydrogels, including pectin-Fe^{3+}/polyacrylamide gels,[36] agar/poly(acrylamide-acrylic acid)-Fe^{3+} gels,[37] agar/poly(acrylic acid) (AAc)-Fe^{3+} gels,[38] alginate-polyacrylamide-Ca^{2+} gels,[39] κ-carrageenan-K^+/polyacrylamide gels,[40] chitosan/poly(acrylic acid) (AAc)-Fe^{3+} gels,[41] and poly(ethylene glycol) (PEG)/poly(acrylamide-acrylic acid) (PAMAAc)-Fe^{3+} gels.[42] However, none of these ionic-cross-linked DN hydrogels has demonstrated their strong surface adhesion on different solid surfaces.

Herein, we reported a fully physical cross-linked Agar/pHEAA[poly(*N*-hydroxyethyl acrylamide)]-AAc-Fe^{3+} DN hydrogel using a simple, one-pot strategy as reported in our previous work,[43] where agar serves as the first network, and pHEAA-AAc-Fe^{3+} serves as the second network. The double networks were associated by multiple, physical bonds, including hydrogen bonds in both networks, AAc-Fe^{3+} ionic interactions in the second pHEAA network, and other physical coordination bonds between the two networks. The synergistic presence of these noncovalent bonds in the DN structure allowed bulk Agar/pHEAA-AAc-Fe^{3+} DN hydrogel to achieve high mechanical properties (fracture stress of 960 kPa, fracture strain of 11, elastic modulus of 600 kPa, tearing energy of 1300 J/m^3, and energy dissipation of 1644 kJ/m^3), as well as high self-recovery, and self-healing properties. Moreover, without any surface modification, Agar/pHEAA-AAc-Fe^{3+} DN hydrogels can also instantly/strongly adhere on not only different solid surfaces (e.g., titanium, glass, aluminum, and ceramics) with high interfacial toughness (2619−4414 J/m^2) but also human skin with repeatable adhesiveness but without causing any damage. Such strong and reversible surface adhesion was likely attributed to the presence of multiple physical interactions of multivalent metal ion complexation, hydrogen bonding, and van der Waals interactions at the hydrogel−surface interface. This work confirms a new physical DN hydrogel with a combination of high mechanical, stretchable, self-recoverable, and surface adhesive properties, which are promising for hydrogel-based adhesive applications such as superglues, coatings, joints, and material−machine interfaces. The working mechanisms for improving both bulk/interfacial toughness could possibly extend to other hydrogels, polymers, or elastomers for different adhesion applications.

EXPERIMENTAL SECTION

Materials. *N*-Hydroxyethyl acrylamide (98.0%, HEAA) was obtained from Tokyo Chemical Industry Co., Ltd. Agar (gel strength >300 g/cm^2), UV-initiator 2-hydroxy-4′-(2-hydroxyethoxy)-2-methylpropiophenone (HMP), and acrylic acid (AAc) (99.0%) were obtained from Sigma-Aldrich. Iron(III) chloride ($FeCl_3$) (98%) and magnesium chloride ($MgCl_2$) (99.0%) were purchased from Alfa Aesar. Calcium chloride ($CaCl_2$) (93%, anhydrous), potassium chloride (KCl) (99.0%), aluminum chloride ($AlCl_3$) (98.5%, anhydrous), and zinc chloride ($ZnCl_2$) were purchased from ACROS, ORGANICS. Carbamide (urea) was purchased from VWR Life Science AMRESCO. Sodium thiocyanate (NaSCN) was obtained from JT Baker Chemical Co. All other chemicals were used as received without extra treatment. Millipore water (resistivity >18.2 MΩ cm) was purified by a purification system.

Preparation of Bulk Hydrogels. Unlike using high-strength agar powers (800 g/cm^2) in the previous work,[44] we purposely selected the much lower-strength agar powders (300 g/cm^2) to prepare Agar/pHEAA-AAc-Fe^{3+} hydrogels. Briefly, 0.24 g of agar, 2 g of HEAA, 0.12 L of AAc, 3 g of $FeCl_3$ aqueous solution (0.68 mol % of AAc), and 0.0428 g of HMP (1 mol % of total monomers) were mixed together with a magnetic stirrer. The solution in the sealed tube was soon heated under

DOI: 10.1021/acsapm.9b00889
ACS Appl. Polym. Mater. 2020, 2, 1031−1042

Scheme 1. Preparation of Agar/pHEAA-AAc-Fe^{3+} DN Gel[a]

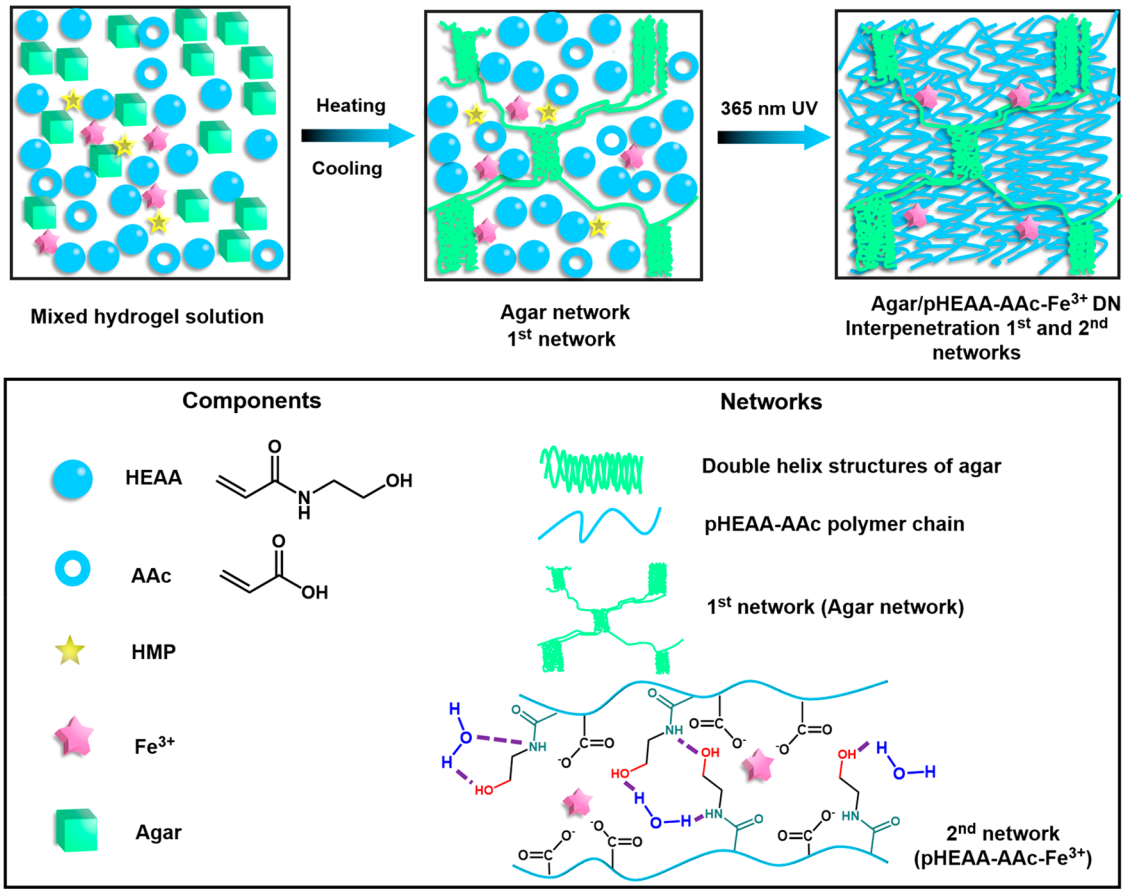

[a]Via a three-step method of heating-cooling-photopolymerization.

boiling water bath. When the mixture solution became transparent, the solution was injected to the mold with pieces of glasses separated by 1 mm thickness of poly(tetrafluoroethylene) (PTFE), and the mold was ultrasonicated to remove the air. After the cooling process, the first agar polysaccharide network formed. Subsequently, the gel in the mold was treated with UV light with a power of 8 W for 1 h of UV polymerization. All other hydrogels, for example, pHEAA-AAc-Fe^{3+} SN and Agar/pHEAA-AAc DN gel with different multivalent metal ions were prepared by the similar method.

Of note, the naming rules of $Agar_a/pHEAA_b$-AAc_c-$Fe^{3+}{}_d$ gels, where a mg/mL of agar to whole system, b weight ratio of HEAA relative to water, c mole percentage of AAc monomer relative to HEAA monomer, and d mole percentage of $FeCl_3$ to AAc monomer. For example, for $Agar_{50}/pHEAA_{2/3}$-AAc_{10}-$Fe^{3+}{}_{0.68}$DN, where the agar concentration was 50 mg/mL to whole system, HEAA weight ratio to water was 2/3, the molar percentage of AAc relative to HEAA was 10, and the mole percentage of Fe^{3+} relative to AAc was 0.68.

Mechanical Measurements. A tensile machine (Instron 3345) was used to examine mechanical properties of the hydrogels. Controlled stretching speed was at 100 mm/min. For the tension test, bulk hydrogel was cut into a dumbbell-shaped sample (25 mm of length, 3.18 mm of width). For loading−unloading hysteresis, a dumbbell-shaped sample was first elongated to a constant strain and then unloaded (50 mm/min). In addition, the hydrogel was cut with a trouser sample (40 mm of length, 20 mm of width, and 20 mm of notch length) with a notch in the middle of the width for tearing test. Subsequently, one arm (width of 10 mm) was fixed by the lower clamp. The other arm (width of 10 mm) was stretched by the upper clamp at a speed of 100 mm/min. Similarly, the cylindrical gel (11 mm of diameter and 15 mm of height) was prepared in a 5 mL injector for compressive measurement. The compressing speed was controlled at 5 mm/min. Moreover, hydrogel samples for 90° peeling test (60 mm of length, 16.5 mm of width, and 3 mm of thickness) were first prepared by special mold. To better fix the back of the gel, Scotch Duct Tape was adhered to the back of the gels by super glue (Loctite) before the 90° peeling test. The gel was peeled from the various substrates (Mecmesin, ACC008-208) at a peeling rate of 150 mm/min.

Self-Healing Tests. The gel with 1 mm of thickness was first cut in half. And then the cross-sectional areas were brought to contact together for 12 h at room temperature or 80 °C. (To avoid inevitable water loss, the hydrogel samples were put and sealed in a transparent plastic bag with 100% humidity.) After it healed, the mechanical property of healed gel was tested by conducting tensile tests at a speed of 100 mm/min.

Scanning Electron Microscopy (SEM). Network morphologies of hydrogels were examined by Hitachi TM3030. Here, fully dried hydrogels were coated with platinum by a sputter-coating machine before the SEM observation (fractured in liquid nitrogen). The cross-sectional area of the gel was chosen and magnified to 1000 times and 4000 times over its original size.

Contact Angle Measurement. Contact angle image was obtained by Rame-Hart model 500 Advanced Goniometer using the Millipore water as the solvent at room temperature. Contact angle was obtained by image analysis with DROP image software. Three positions in each substrate were chosen to obtain mean and standard deviation.

Swelling Ratio Measurement. The cylindrical gels (diameter: 8 mm; thickness: 1 mm) were fully swollen in Millipore water, urea solution (5 M), and NaSCN solution (5 M). Prior to weighing, water on surfaces was wiped away. The equilibrium swelling ratio was expressed as $g_s = m_w/m_0$, where m_w was the weight of the gel at the swollen state, and m_0 was the weight of as-prepared gel.

DOI: 10.1021/acsapm.9b00889
ACS Appl. Polym. Mater. 2020, 2, 1031−1042

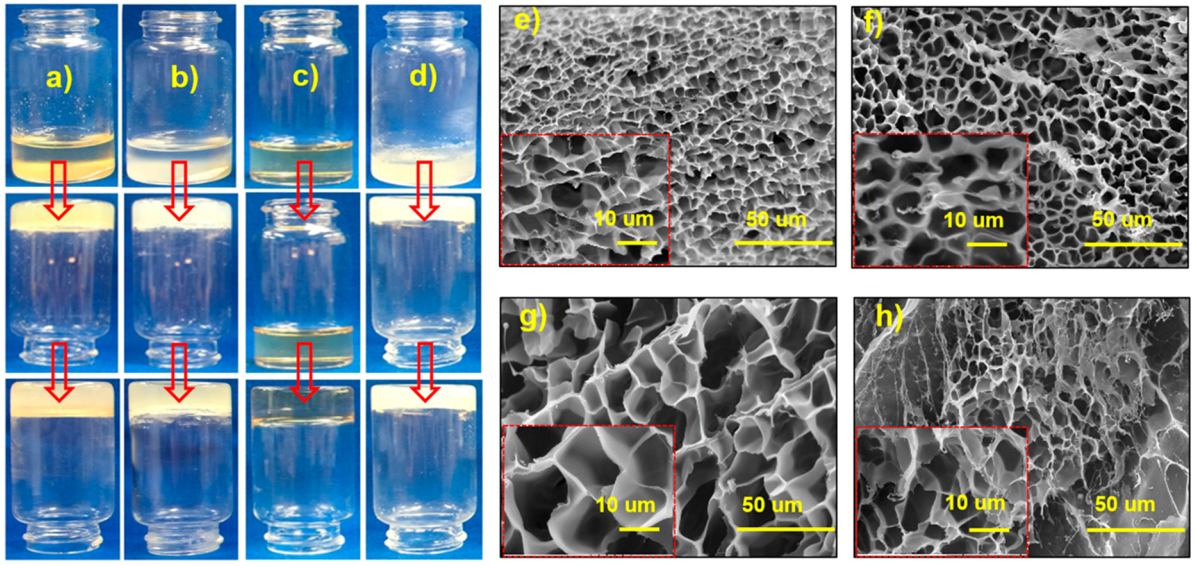

Figure 1. Gelation process of (a) Agar/pHEAA-AAc-Fe^{3+}DN gel, (b) Agar/pHEAA-AAc DN gel, (c) pHEAA-AAc-Fe^{3+} SN gel, and (d) Agar SN gel. SEM images of (e) Agar/pHEAA-AAc-Fe^{3+}DN gel, (f) Agar/pHEAA-AAc DN gel, (g) pHEAA-AAc-Fe^{3+} SN gel, and (h) Agar SN gel.

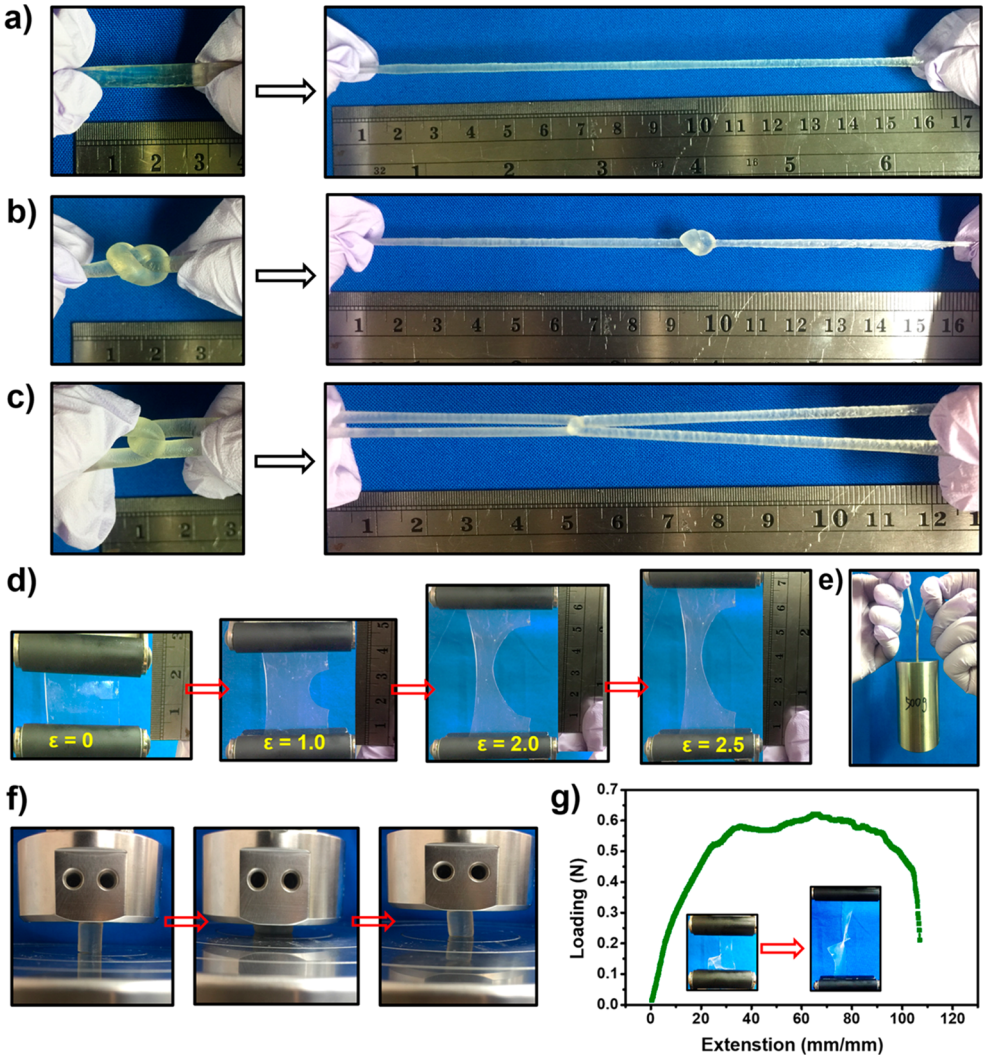

Figure 2. Great mechanical behaviors of Agar/pHEAA-AAc-Fe^{3+} DN gels. (a) Direct, (b) knotted, (c) crossover stretching to ~6 times their initial length, (d) resist crack propagation, (e) hold a weight (500 g), (f) endure compression deformation, and (g) a tearing force vs displacement curve.

DOI: 10.1021/acsapm.9b00889
ACS Appl. Polym. Mater. 2020, 2, 1031−1042

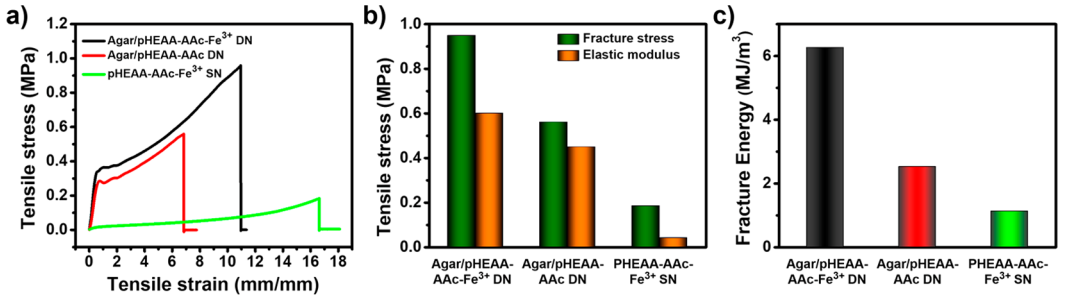

Figure 3. Tensile properties of Agar/pHEAA-AAc-Fe^{3+} DN gel, Agar/pHEAA-AAc DN gel, and pHEAA-AAc-Fe^{3+}SN gel, as characterized by (a) stress−strain curves, (b) fracture stress and elastic modulus, and (c) fracture energy.

RESULTS AND DISCUSSION

Preparation and Characterizations of Agar/pHEAA-AAc-Fe^{3+}DN Gels. Scheme 1 shows a three-step preparation of Agar/pHEAA-AAc-Fe^{3+} DN gels via a heating-cooling-photopolymerization process. Briefly, all reactants of agar, acrylic acid, *N*-hydroxyethyl acrylamide, HMP, and $FeCl_3$ were dissolved in a well-mixed solution, then heated to 95 °C under continuous stirring, during which powder-like agar molecules changed themselves to linear-like agarose macromolecular chains, resulting in a transparent solution. Next, the transparent mixture solution was gradually cooled to room temperature, during which agarose macromolecular chains underwent structural transition from linear to helical conformations, followed by aggregation of helical agarose chains into helical bundles, leading to the formation of the first agar network. After that, UV light was introduced to polymerize the second pHEAA-AAc-Fe^{3+} network that interpenetrates with the first agar network, forming an Agar/pHEAA-AAc-Fe^{3+} DN gel. During the whole preparation process, since no chemical cross-linker was added in the system, both networks in Agar/pHEAA-AAc-Fe^{3+} DN gels were physically cross-linked by multiple noncovalent bonds; that is, the first agar network was cross-linked by hydrogen bonds between agar helical bundles, while the second pHEAA-AAc-Fe^{3+} network was cross-linked by hydrogen bonds between hydrophilic amide and hydroxyl groups and ionic interactions between AAc-Fe^{3+}.

Figure 1a−d shows a general gelation process for Agar/pHEAA-AAc-Fe^{3+}DN (Figure 1a), Agar/pHEAA-AAc DN (Figure 1b), pHEAA-AAc-Fe^{3+} SN (Figure 1c), and Agar SN hydrogels (Figure 1d) at the initial, heating−cooling, and UV polymerization stages. Visual inspection showed that, through the three-step polymerization, each of the four gels was successfully formed but with different appearances; that is, the gels with Fe^{3+} ions showed a brownlike color, while the gels without Fe^{3+} ions had a milky color. Furthermore, SEM images in Figure 1e−h show the morphologies and microstructures of Agar/pHEAA-AAc-Fe^{3+} DN (Figure 1e), Agar/pHEAA-AAc DN hydrogels (Figure 1f), pHEAA-AAc-Fe^{3+} SN gel (Figure 1g), and Agar SN gel (Figure 1h). Overall, while all gel samples exhibited spongelike and continuous porous structures in cross-sectional areas, four different gels had different pore size distributions. Both Agar/pHEAA-AAc-Fe^{3+} (2−6 μm) and Agar/pHEAA-AAc (4−8 μm) DN gels had the smaller pore sizes than pHEAA-AAc-Fe^{3+} (9−11 μm) and Agar (3−8 μm) SN gels. This indicates that DN structure enables to achieve a much denser 3D network structure than SN structure, and the presence of AAc-Fe^{3+} can further tighten the network structure via the attractive electrostatic interactions, leading to the more compact structure.

Mechanical Properties of Agar/pHEAA-AAc-Fe^{3+} DN Gels. At first glance in Figure 2a−c, Agar/pHEAA-AAc-Fe^{3+} DN gels were highly stretchable to withstand straight stretching, crossover stretching, and knotted stretching up to ∼6 times of initial states without fracture. In Figure 2d, a notched Agar/pHEAA-AAc-Fe^{3+} DN gel showed a strong resistance against the crack propagation up to a final strain of 2.5. Agar/pHEAA-AAc-Fe^{3+} DN gels can also hold a weight of 0.5 kg (Figure 2e) and endure a compression stress of 1.21 MPa (70% of strain) (Figure 2f). Upon release of compression force, the gel recovered immediately to its original shape, indicating that Agar/pHEAA-AAc-Fe^{3+} DN gel possesses a shape-recovery property after a large network deformation. Figure 2g illustrated a typical tearing curve of Agar/pHEAA-AAc-Fe^{3+} DN gel, whose tearing energy was 1306 J/m^2 comparable to articular cartilage and G4· K^+/PDMAAm DN gels.[45]

Further, we performed tensile tests to measure and compare the mechanical properties of Agar/pHEAA-AAc-Fe^{3+} DN, Agar/pHEAA-AAc DN, and pHEAA-AAc-Fe^{3+} SN hydrogels. Agar SN was too weak to be tested. The preparation conditions and mechanical properties [fracture stress (σ), fracture strain (λ), elastic modulus (E), and fracture energy (W_σ)] of these gels were summarized in Table S1. Specifically, Figure 3a−c showed that Agar/pHEAA-AAc-Fe^{3+}DN gel (σ of 0.96 MPa, λ of 11 mm/mm, E of 0.60 MPa, W_σ of 6.28 MJ/m^3) showed the best mechanical properties, as compared to Agar/pHEAA-AAc DN gel (σ of 0.56 MPa, λ of 6.83 mm/mm, E of 0.45 MPa, W_σ of 2.52 MJ/m^3) and pHEAA-AAc-Fe^{3+} SN gel (σ of 0.19 MPa, λ of 16.6 mm/mm, E of 0.04 MPa, W_σ of 1.12 MJ/m^3). The results reveal that the introduction of Fe^{3+}-AAc ionic interactions into the second network can indeed act as additional, reversible sacrificial bonding to dissipate energy efficiently, thus conferring high mechanical performances to Agar/pHEAA-AAc-Fe^{3+} DN hydrogel.

Intuitively, hydrogel components are the key factors for determining the mechanical performances of hydrogels. Since our previous work has examined the concentration effects of Agar and HEAA on mechanical performances of Agar/pHEAA DN hydrogels, here we mainly studied the ionic cross-linker effects of AAc (Figure S1) and Fe^{3+} (Figure S2) on mechanical performances of Agar/pHEAA-AAc-Fe^{3+} DN gel. Regarding AAc effect, the hydrogel showed an optimal AAc concentration of 10 mol % of HEAA to achieve the best mechanical properties. As shown in Figure S1a−c, with a gradual increase in AAc contents from 0 to 10 mol % of HEAA, Agar/pHEAA-AAc-Fe^{3+} DN gels increased their fracture stress from 0.48 to 0.96 MPa, elastic modulus from 0.36 to 0.60 MPa, and fracture energy from 2.64 to 6.28 MJ/m^3, respectively. However, further increase of AAc content from 10 to 20 mol % led to decrease of fracture

DOI: 10.1021/acsapm.9b00889
ACS Appl. Polym. Mater. 2020, 2, 1031−1042

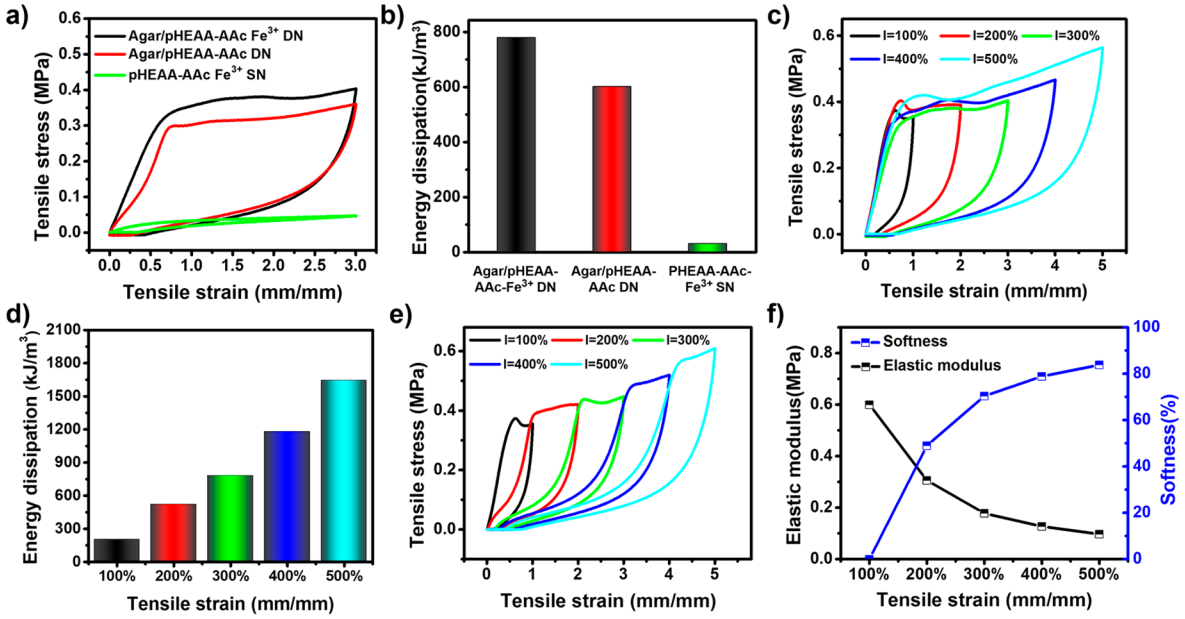

Figure 4. (a) Hysteresis loop and (b) energy dissipation of Agar/pHEAA-AAc-Fe^{3+} DN, Agar/pHEAA-AAc DN, and pHEAA-AAc-Fe^{3+}SN hydrogels at λ = 3 using a loading−unloading test. (c) Hysteresis loop and (d) energy dissipation of different Agar/pHEAA-AAc-Fe^{3+} DN gels at changeable tensile strains using cyclic loading−unloading tests. (e) Hysteresis loop and (f) elastic modulus and softness of the same Agar/pHEAA-AAc-Fe^{3+} DN gels at different strains via successive loading−unloading measurements.

stress from 0.96 to 0.75 MPa, fracture strain from 11.00 to 9.7, and fracture energy from 6.28 to 4.22 MJ/m^3. Similarly, there also existed an optimal concentration of Fe^{3+} (0.68 mol % of AAc) to achieve the best mechanical properties of σ of 960 kPa, λ of 11 mm/mm, E of 600 kPa, and W_σ of 6.28 MJ/m^3(Figure S2a−c). Clearly, too low or too high concentrations of AAC or Fe^{3+} will reduce the mechanical performance of DN hydrogels, suggesting AAC and Fe^{3+} function as typical cross-linkers to alter network structures and subsequent mechanical properties. On one hand, low concentrations of AAc or Fe^{3+} will lead to insufficient ionic coordination to be formed between AAc and Fe^{3+}, thus not enhancing network association and mechanical properties. On the other hand, excessive AAc or Fe^{3+} concentrations will also cause a typical over-cross-linking issue, which shortens effective chain lengths in the networks, restricts chain flexibility, and induces more network inhomogeneity, all of which would reduce energy dissipation and make the gels to be fractured easily at low strains. Overall, Agar/pHEAA-AAc-Fe^{3+} DN hydrogels exhibited the top mechanical performance with Fe^{3+} of 0.68 mol % of AAc, agar of 50 mg/mL, HEAA of 2/3 mass ratio of water, and AAc of 10 mol % of HEAA. Unless stated otherwise, such optimal conditions were used for preparing our Agar/pHEAA-AAc-Fe^{3+} DN gels for further tests.

High toughness, strength, and fracture energy of Agar/pHEAA-AAc-Fe^{3+} DN gels are likely attributed to multiple physical bonds such as hydrogen bonds within and between two networks and AAc-Fe^{3+} ionic coordination in the second network. We also prepared different Agar/pHEAA-AAc-K^+, Agar/pHEAA-AAc-Mg^{2+}, Agar/pHEAA-AAc-Zn^{2+}, Agar/pHEAA-AAc-Ca^{2+}, and Agar/pHEAA-AAc-Al^{3+} by introducing different cationic ions (K^+, Ca^{2+}, Zn^{2+}, Al^{3+}) to coordinate with AAc in the Agar/pHEAA networks. In Figure S3a−d, the resultant hydrogels exhibited tensile properties (σ of 430−510 kPa, λ of 5.09−7.78, E of 260−430 kPa, W_σ of 1.68−2.50 MJ/m^3), similar to those of Agar/pHEAA-AAc hydrogels (σ of 560 kPa, λ of 6.83, E of 450 kPa, W_σ of 2.52 MJ/m^3) but not better than those of Agar/pHEAA-AAc-Fe^{3+} hydrogels. Generally speaking, metal−carboxylate interactions are strongly related to the number of metal coordination bonds for ionic cross-linking process of polymer chains containing a large amount of carboxylate groups.[37] On the one hand, at the coordination equilibrium, the higher cationic valence, the more metal−carboxylate coordination bonds. Thus, trivalent ions (Al^{3+} and Fe^{3+}) usually have stronger coordination effect than bivalent (Mg^{2+}, Zn^{2+}, Ca^{2+}) and univalent ions (K^+ and Na^+). On the other hand, a number of studies have also shown that ionic coordination effect also depends on local environments (e.g., pH, solvent).[46,47] Here, pH locally generated by Fe^{3+}-carboxyl groups would enhance the stability of metal coordination bonds, which in turn achieve the higher binding strength and mechanical properties than Al^{3+}-carboxyl groups. A similar effect of metal-coordination complexes on the mechanical properties of poly(AAm-co-AAc) hydrogels was also reported with a decreased mechanical enhancement order of Fe^{3+} > Al^{3+} > Zn^{2+} > Ca^{2+} > Mg^{2+}.[48]

Mechanical Recovery of Agar/pHEAA-AAc-Fe^{3+} DN Gels. To better comprehend the role of ionic cross-linking effect in energy dissipation, different successive loading−unloading measurements on Agar/pHEAA-AAc-Fe^{3+} DN gel, Agar/pHEAA-AAc DN gel, and pHEAA-AAc-Fe^{3+} SN gel were conducted. First, as shown in Figure 4a,b, at λ = 3, Agar/pHEAA-AAc-Fe^{3+} DN gel displayed the largest hysteresis loop, as compared to pHEAA-AAc-Fe^{3+} SN gel and Agar/pHEAA-AAc DN gel. The associated energy dissipation was 780 kJ/m^3 for Agar/pHEAA-AAc-Fe^{3+} gel, 601 kJ/m^3 forAgar/pHEAA-AAc DN gel, and 29.2 kJ/m^3 for pHEAA-AAc-Fe^{3+} gel, respectively. Clearly, the introduction of AAc-Fe^{3+} into the second network allows to dissipate energy in a much more efficient way. Also, both DN hydrogels with and without Fe^{3+} ions also showed superior performance to pHEAA-AAc-Fe^{3+}SN, indicating the significance and effectiveness of DN as a mechanical property enhancer.

DOI: 10.1021/acsapm.9b00889
ACS Appl. Polym. Mater. 2020, 2, 1031−1042

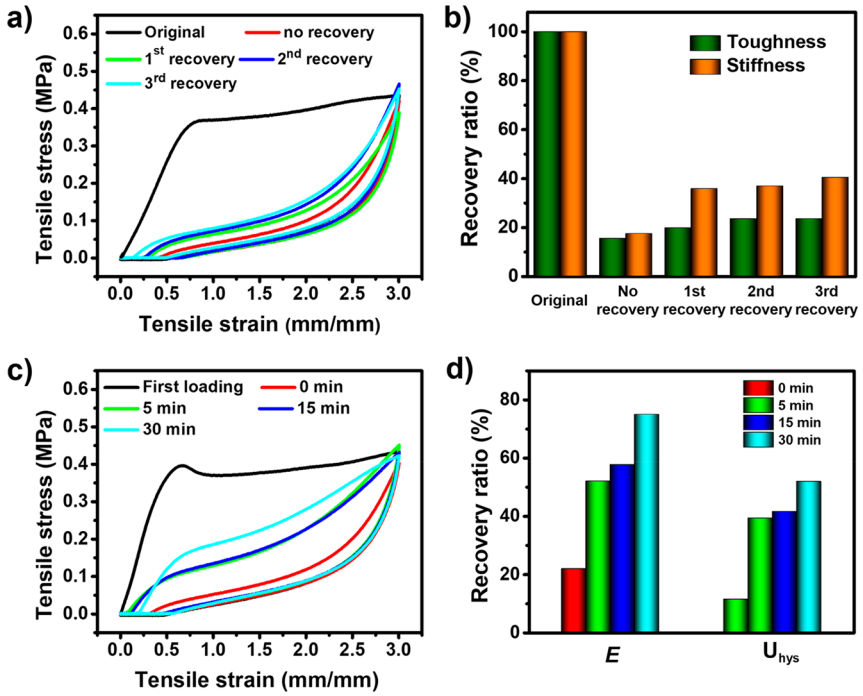

Figure 5. Mechanical recovery of Agar/pHEAA-AAc-Fe^{3+} DN gel via cyclic loading−unloading measurements. (a, c) Hysteresis loops and (b, d) the corresponding toughness/recovery ratios of the gel with different resting intervals (a, b) at 25 °C and (c, d) at 80 °C. Stiffness and toughness recovery of the hydrogels are calculated from hysteresis curves.

Next, we performed cyclic loading−unloading tests on different Agar/pHEAA-AAc-Fe^{3+} DN gels prepared under the same condition at different strains. As shown in Figure 4c,d, hysteresis loops increased with strains, so that the dissipated energy monotonically increased from 202 to 1644 kJ/m^3 as strains increased from 1 to 5. The cyclic loading−unloading tests on different Agar/pHEAA-AAc-Fe^{3+} gels demonstrates that energy dissipation not only depends on the loading strains but also becomes more efficient as the hydrogel is subject to large strains, indicating that physical interactions in both networks can work together to endure high deformation and to dissipate energy efficiently. Furthermore, we conducted a successive loading−unloading test on the same Agar/pHEAA-AAc-Fe^{3+} DN hydrogel to study its internal fracture process at different strains in Figure 4e,f. No resting time was applied to the same gel between any two consecutive loading cycles. On the one hand, stiffness of hydrogel decreased continuously from 0.6 to 0.1 MPa, while softness gradually increased from 0 to 83.79% as strains increased from 1 to 5, indicating that the softening behavior of the gel occurs far below the yield point and continues to spread with increasing elongations. On the other hand, we also observed some small overlap regions between any adjacent hysteresis loops. This indicates a partial recovery of the networks in Agar/pHEAA-AAc-Fe^{3+} DN gel.

Because of the presence of multiple, reversible noncovalent bonds (e.g., hydrogen bonds and ionic interactions) in both networks, mechanical self-recovery is expected from Agar/pHEAA-AAc-Fe^{3+} DN gel. Here, we examined the self-recovery property of Agar/pHEAA-AAc-Fe^{3+} DN gel via five loading−unloading cycles at $\lambda = 3$ and room temperature. There was no resting interval between the first and second cycles, but there was 30 min of resting for the third, fourth, and fifth cycles. During the first cycle, Agar/pHEAA-AAc-Fe^{3+} DN hydrogel showed a relatively big loop with the energy dissipation at 780 J/m^2, which was much higher than that of Agar/pHEAA-AAc DN (602 J/m^2) and pHEAA-AAc-Fe^{3+} SN hydrogels (29.2 J/m^2). In the immediate second cycle, the three hydrogels exhibited smaller hysteresis loops and reduced their hysteresis energy to 123, 64.5, 13.6 J/m^2, respectively (Figure S4), implying that reversible noncovalent bonds could not be largely recovered without resting. So, to improve the self-recovery property of Agar/pHEAA-AAc-Fe^{3+} DN gel, we applied a 30 min rest for each following cycle. It can be seen in Figure 5a,b that, upon resting for 30 min during the third to fifth cycles, Agar/pHEAA-AAc-Fe^{3+} DN gels increased their toughness/recovery ratios from 15.3/17.3% in the second cycle to 19.6/35.7%, 23.4/36.8%, and 23.4/40.3% in the third, fourth, and fifth cycles. The longer resting time definitely would help to reform ionic association and hydrogen bonding in both networks. To understand the role of AAc-Fe^{3+} ionic cross-linking in self-recovery of Agar/pHEAA-AAc-Fe^{3+} DN gel, we further tested Agar/pHEAA-AAc DN gel without Fe^{3+} by five cycles at the same conditions. Without Fe^{3+}, Agar/pHEAA-AAc DN gels could recover their toughness/stiffness ratio to 20/37.6%, 18/36.4%, and 18.2/37.1% for the third, fourth, and fifth cycles, respectively (Figure S5). It appears that the introduction of AAc-Fe^{3+} can slightly improve toughness/stiffness recovery by 3−5% for the second pHEAA network.

Considering that the second network recovery as contributed by AAc-Fe^{3+} association is rather limited at room temperature, it is necessary to improve the overall mechanical self-recovery by reconstructing the first agar network at a sol−gel temperature of 80 °C. As shown in Figure 5c, the hysteresis loops gradually increased as time passed, showing a good self-recovery behavior at 80 °C. Accordingly, the toughness/stiffness recovery ratio became 52/39.3%, 57.7/41.6%, and 75/51.9% after 5, 15, and 30 min of resting at 80 °C (Figure 5d). Evidently, by reconstructing agar helical bundles at 80 °C, Agar/pHEAA-AAc-Fe^{3+}DN gel can recover its toughness/stiffness as high as 75/52%. Side-by-side comparison of toughness/stiffness recovery between

DOI: 10.1021/acsapm.9b00889
ACS Appl. Polym. Mater. 2020, 2, 1031−1042

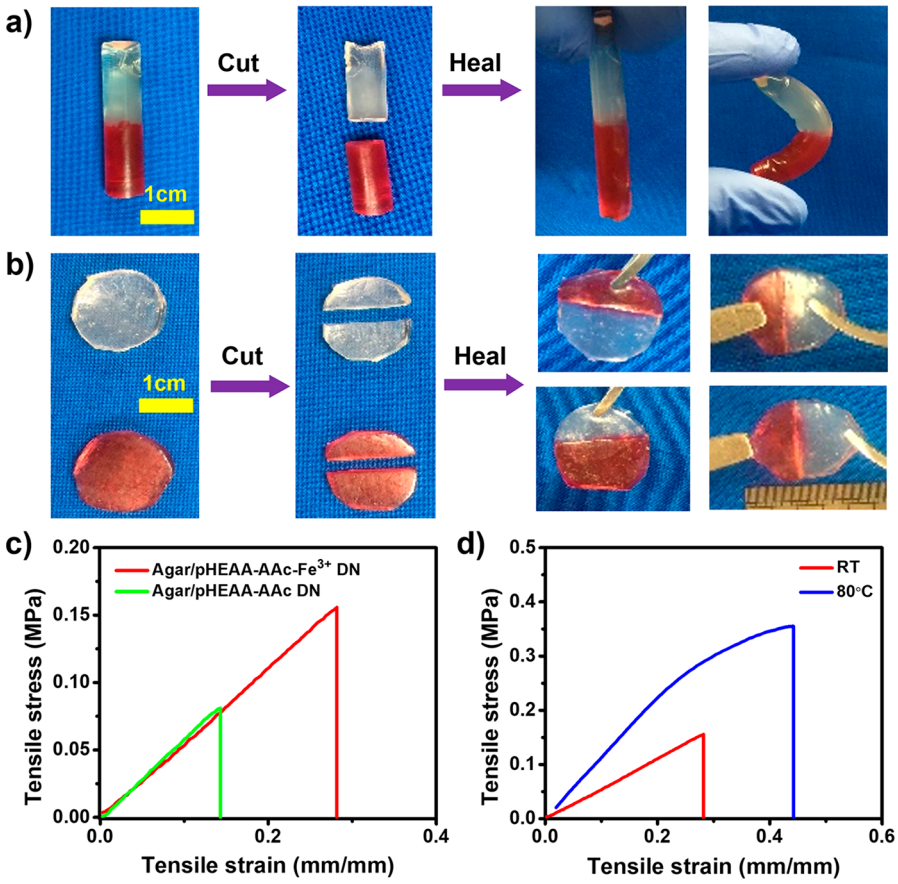

Figure 6. Self-healing of Agar/pHEAA-AAc-Fe^{3+} DN gels. Visual inspection of the healed gels to sustain (a) bending and (b) stretching after 12 h of healing at room temperature. Stress−strain curves of (c) the healed Agar/pHEAA-AAc-Fe^{3+} DN gel and Agar/pHEAA-AAc DN gel at 25 °C and (d) the healed Agar/pHEAA-AAc-Fe^{3+} DN gels at room temperature and 80 °C. Scale bar: 1 cm.

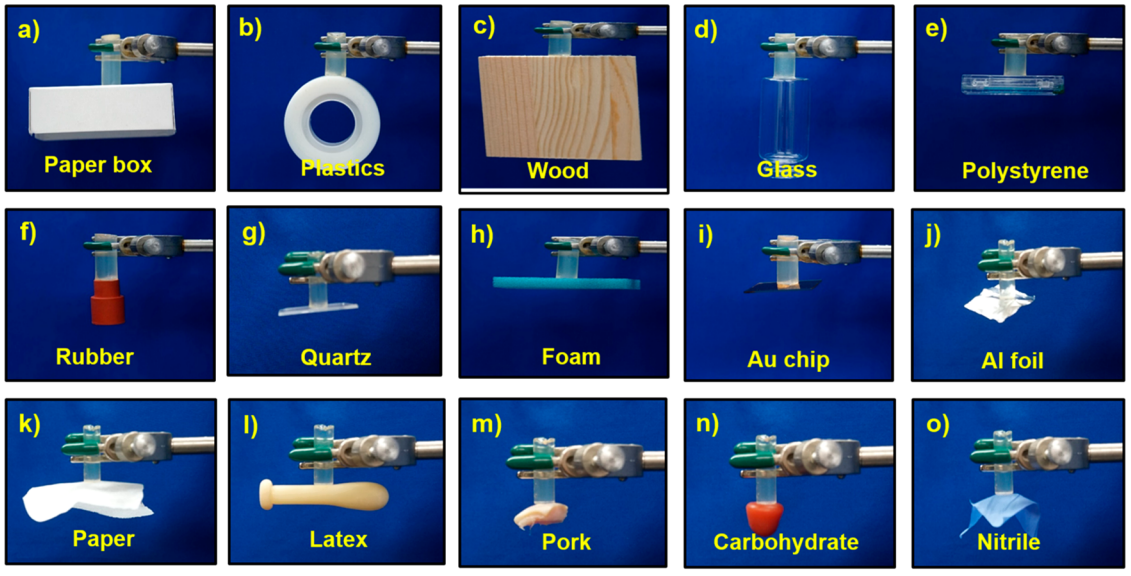

Figure 7. Demonstration of adhesion performances of Agar/pHEAA-AAc-Fe^{3+} DN gels on various (a−j) hard and (k−o) soft surfaces.

different hydrogels with and without Fe^{3+} and at different temperatures confirms that hydrogel bonds and ionic association work together to improve the mechanical recovery of Agar/pHEAA-AAc-Fe^{3+} gel.

As opposite to self-recovery tests, we also designed the experiments to destroy H-bonds and ionic interaction by immersing Agar/pHEAA-AAc-Fe^{3+} DN gel into Millipore water, urea (5 M), and NaSCN (5 M) solutions, all of which were hydrogen-bond-breaking reagents. Agar/pHEAA-AAc-Fe^{3+} swelled significantly in three solutions, achieving the equilibrium swelling ratio of 7.02 in Millipore water, 19.21 in urea solution (5 M), and ∼32.04 in NaSCN solution (5 M) (Figure S6a).

DOI: 10.1021/acsapm.9b00889
ACS Appl. Polym. Mater. 2020, 2, 1031−1042

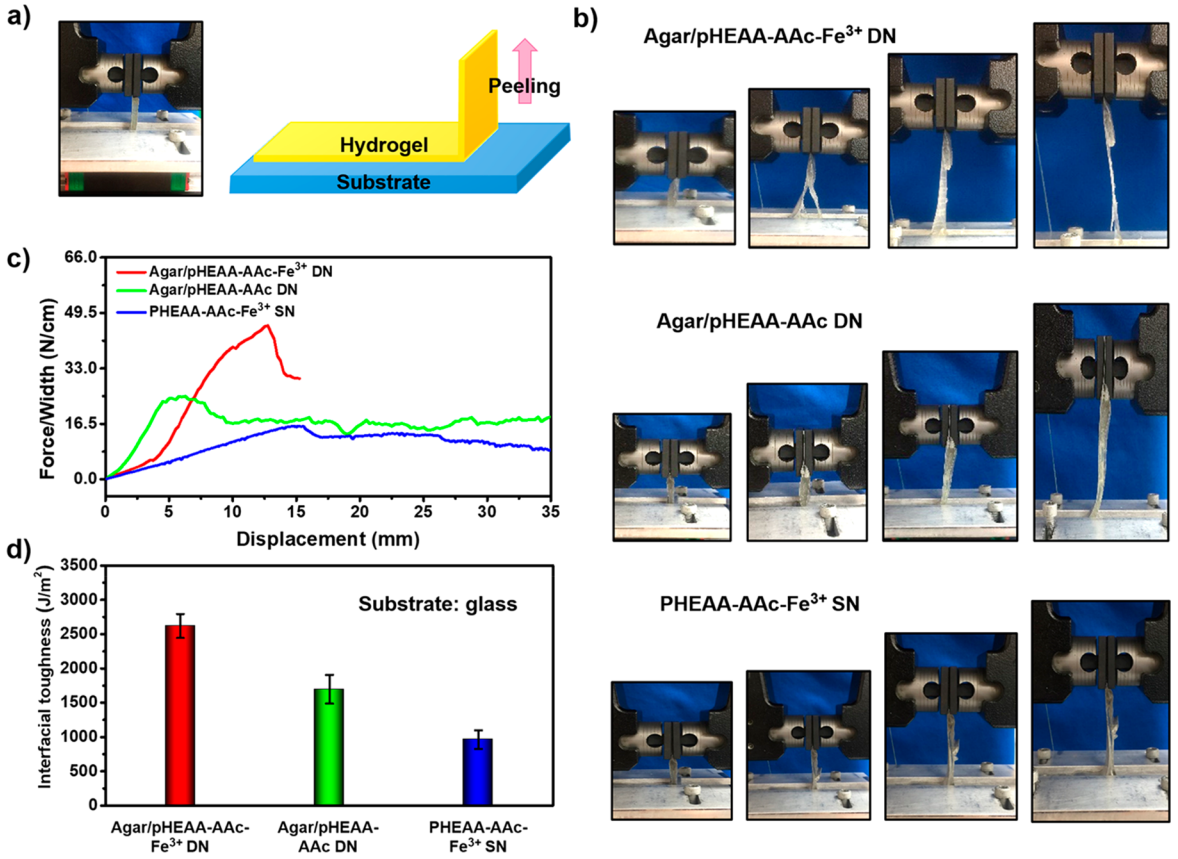

Figure 8. (a) Typical model of 90° peeling test. (b) Peeling-off process of Agar/pHEAA-AAc-Fe^{3+} DN, Agar/pHEAA-AAc DN, and pHEAA-AAc-Fe^{3+} SN hydrogel from the smooth glass substrate. (c) Force−displacement curves and (d) interfacial toughness of the above three gels onto glass substrate.

Increase of swelling ratio is an indicator of the destruction of H-bonds in urea solution but both H-bonds and ionic interactions in NaSCN solution, leading to a larger expansion of network. Additionally, the ionic interactions between COO^- and Fe^{3+} ions are strongly influenced by pH value. From this perspective, NaSCN solution indeed promotes the destruction of the internal physical cross-linked structures of hydrogel. As expected, all swollen hydrogels significantly reduced their mechanical properties. As shown in Figure S6b, Agar/pHEAA-AAc-Fe^{3+} DN reduced the tensile stress/strain to 0.11 MPa/5.4 mm/mm in water, 0.04 MPa/4.0 mm/mm in urea, and 0.009 MPa/2.0 mm/mm in NaSCN, respectively, further explaining an important role of physical cross-links of H-bonds and ionic interactions in hydrogel mechanical properties.

Self-Healing of Agar/pHEAA-AAc-Fe^{3+} DN Gels. Because of the reversible physical cross-linking properties, we also tested the self-healing performance of Agar/pHEAA-AAc-Fe^{3+} DN gels. Figure 6a showed the cylindrical gel was cut in half and brought together for 12 h at 25 °C. After 12 h, the cut pieces can heal together and bend to 60°. Further, the cut pieces from different gels can also heal together at room temperature for 12 h, and the healed gels can sustain stretching by a tweezer (Figure 6b). Quantitively, a tensile test was conducted to evaluate the self-healing efficiency of Agar/pHEAA-AAc-Fe^{3+} DN gels. The healed Agar/pHEAA-AAc-Fe^{3+} DN gel (σ of 0.16 MPa, λ of 0.3 mm/mm, W_σ of 0.024 MJ/m^3) showed the higher mechanical properties than the healed Agar/pHEAA-AAc DN (σ of 0.078 MPa, λ of 0.154 mm/mm, W_σ of 0.0069 MJ/m^3) (Figure 6c). To heal the hydrogel at elevated temperature of 80 °C, the healed Agar/pHEAA-AAc-Fe^{3+} DN gel further improved its mechanical property to σ of 0.11 MPa, λ of 0.48 mm/mm, and W_σ of 0.108 MJ/m^3, as compared to the healed gel at room temperature (Figure 6d).

Interfacial Toughness of Agar/pHEAA-AAc-Fe^{3+} DN Gels. Given the reversible physical cross-linking in the ionic DN gel, Agar/pHEAA-AAc-Fe^{3+} DN gel exhibited a general and strong adhesion on a wide range of hard surfaces, including paper box, plastics, wood, glass, polystyrene, rubber, quartz, foam, golden chip, and aluminum foil (Figure 7a−j), as well as soft surfaces including paper, latex, pork, carbohydrate, and nitrile (Figure 7k−o). Additionally, Agar/pHEAA-AAc-Fe^{3+} gel exhibited repeatable and durable adhesion on different positions of human arms without damage or pain (data not shown). The durable adhesive of the hydrogel was attributed to the presence of a sufficient number of hydrogen bonds in dual networks and ionic cross-linkers in the second network.

Interfacial toughness between the Agar/pHEAA-AAc-Fe^{3+} hydrogel and glass was measured by the 90° peeling test in Figure 8a. Visual inspection in Figure 8b exhibited that (i) Agar/pHEAA-AAc-Fe^{3+} hydrogel showed higher adhesion on the glass than Agar/pHEAA-AAc DN and pHEAA-AAc-Fe^{3+} SN hydrogels, as evidenced by a larger stripping lag during the peeling process and a larger amount of residual gel after the peeling process and (ii) Agar/pHEAA-AAc-Fe^{3+} DN gel can be easily yet completely peeled off from the glass substrate; instead, the gels were broken before peeling off the glass, suggesting that interfacial toughness of Agar/pHEAA-AAc-Fe^{3+} DN gel is stronger than its bulk toughness. In Figure 8c,d, the measured interfacial energy of this DN gel on the glass was 2619 J/m^2, which was 1.5 and 2.5 times higher than that of Agar/pHEAA-

DOI: 10.1021/acsapm.9b00889
ACS Appl. Polym. Mater. 2020, 2, 1031−1042

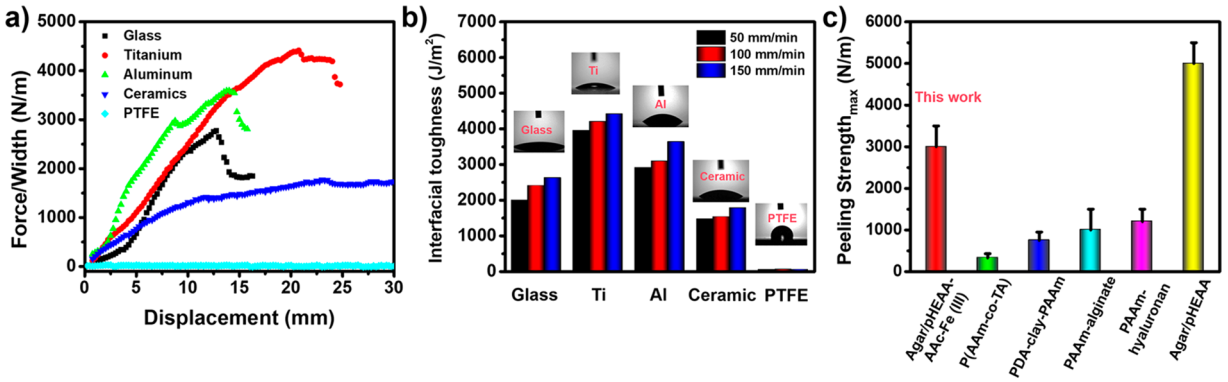

Figure 9. (a) Peeling curves of Agar/pHEAA-AAc-Fe^{3+} DN gels on various substrates such as glass, titanium, aluminum, ceramics, and PTFE (peeling rate of 50 mm/min) and (b) interfacial toughness of Agar/pHEAA-AAc-Fe^{3+} DN gels on various nonporous solid substrates (control peeling rates of 50−150 mm/min, as well as corresponding water contact angles). (c) Comparison of maximum adhesion strength between our and other adhesive hydrogels.

AAc DN (1697 J/m^2) and pHEAA-AAc-Fe^{3+} SN hydrogels (962 J/m^2). Agar SN hydrogel was easily removed from glass indicating almost negligible surface adhesion. Strong adhesion energy of Agar/pHEAA-AAc-Fe^{3+} DN gel over others is likely attributed to the addition of ionic AAc-Fe^{3+} cross-linker to improve interfacial toughness between the glass and hydrogels. We also immersed Agar/pHEAA-AAc-Fe^{3+} DN gel with glass into Millipore water, urea solution (5 M), and NaSCN solution (5 M), separately. After immersion, the measured interfacial energy of Agar/pHEAA-AAc-Fe^{3+} DN gel on glass was reduced to 1354, 811, and 56 J/m^2 in Millipore water, urea solution (5 M), and NaSCN solution (5 M), respectively (Figure S7). Agar/pHEAA-AAc-Fe^{3+} DN gel can still retain very high interfacial toughness in wet water and urea conditions, but it almost completely lost its interfacial toughness in NaSCN solution, further highlighting the important role of H-bonds and ionic interactions in enhancing the interfacial toughness of this DN gel on solid surface.

Next, we explored the adhesion behaviors of Agar/pHEAA-AAc-Fe^{3+} DN gels on different solid surfaces. Figure 9a exhibited that as-prepared Agar/pHEAA-AAc-Fe^{3+} DN gels also exhibited high adhesion energy of 4414 J/m^2 on Ti sheet, 3631 J/m^2 on Al sheet, 1773 J/m^2 on ceramics, and 2619 J/m^2 on glass at a peeling rate of 50 mm/min, respectively. Different adhesion strength of Agar/pHEAA-AAc-Fe^{3+} DN gels on various solid surfaces may derive from their different physical interactions at hydrogel−solid interfaces. We further varied the peeling rate from 50 to 150 mm/min, the interfacial toughness of gel-glass, gel-titanium, gel-aluminum, and gel-ceramics, respectively, increased from 1985 to 2619 J/m^2, from 3948 to 4414 J/m^2, from 2907 to 3631 J/m^2, and from 1461 to 1773 J/m^2 (Figure 9b), suggesting the rate-dependent energy dissipation behavior that could be caused by the viscoelasticity of Agar/pHEAA-AAc-Fe^{3+} DN gels. To examine the role of hydrogen bonds in surface adhesion of hydrogels, we conducted the peeling tests of Agar/pHEAA-AAc-Fe^{3+} gel on a hydrophobic PTFE surface. The peeling test showed that Agar/pHEAA-AAc-Fe^{3+} DN gel can be easily removed from the hydrophobic PTFE surface, with a very low interfacial toughness of 42 J/m^2. This result appears to suggest a correlation between interfacial toughness and surface hydrophilicity, because hydrophobic PTFE surface can prevent the formation of hydrogen bonds between the gel and surface. As shown in Figure 9b (inset pictures), the hydrophilic substrates (glass, titanium, aluminum, and ceramics) exhibited relatively low contact angles from 27.5 to 41.4°, while the PTFE showed a much higher contact angle at 108.9°. These results confirm that hydrophilic solid surfaces enable to form strong metal coordination, hydrogen bonding, and ionic interaction with hydrogels, thus leading to high interfacial toughness. Figure 9c shows a comparison of maximum adhesion strength between our and other hydrogel systems. It can be seen that traditional adhesive hydrogels of poly(AAm-co-acrylated thymine[49] and PDA-clay-PolyAAm[50]) showed less than 1000 N/m of peeling strength, while PAAm-alginate and PAAm-hyaluronan[32] exhibited 1000−2000 N/m of peeling strength. For comparison, Agar/pHEAA-AAc-Fe^{3+} hydrogel exhibited the average peeling strength of 3000 N/m superior to the above-mentioned classical hydrogel adhesives. Of note, Agar/pHEAA-AAc-Fe^{3+} hydrogels prepared by the low-strength agar powers (300 g/cm^2) exhibited lower peeling strength than Agar/pHEAA hydrogels prepared by the high-strength agar powers (800 g/cm^2).[44]

Different from self-recoverable or self-healing behavior of tough hydrogels in bulk phase, reversible surface adhesion of tough hydrogels to different surfaces requires additional efforts to re-establish the interfacial interactions between hydrogels and surfaces, and this becomes even more challenging if a rapid and reversible surface adhesion is needed for some surface adhesion applications. After the first peeling off, it is inevitable for any surface to be modified by the adhered and fractured hydrogel residues, which in turn affect the physicochemical properties of the surface and interfacial interactions between hydrogel and surface. Moreover, the subsequent readhesion of hydrogel on the surface can not completely exclude tiny air bubbles at hydrogel−surface interface, which further weaken interfacial interactions. Thus, inevitable air gap and fractured tiny hydrogel residues are the two main factors to largely reduce interfacial interactions and surface adhesion energy of hydrogels on surfaces. It is also aware in some cases that, after the second peeling test, these two factors remained almost unchanged, so did the adhesion energy of hydrogels. To remedy this issue, we proposed two general strategies for improving or introducing reversible surface adhesion of hydrogels to surfaces. For the physical hydrogels without stimuli-responsive properties, design strategies need consideration to incorporate multiple and synergistic physical bonds in the hydrogels, so that the combination of these physical bonds would be sufficient enough to contribute to reversible surface adhesion as needed for specific applications. For the stimuli-responsive hydrogels, the design strategies need to introduce a simple or straightforward

DOI: 10.1021/acsapm.9b00889
ACS Appl. Polym. Mater. 2020, 2, 1031−1042

stimulus (i.e., solvent washing, white light, mild heating) to rapidly recover the surface adhesion of hydrogels to surfaces.

CONCLUSIONS

In conclusion, we developed a fully physical cross-linked double network hydrogel of Agar/pHEAA-AAc-Fe^{3+} to realize a combination of high strength, stiffness, self-recovery, and surface adhesion. By carefully constructing multiple and reversible physical bonds in double network structure, Agar/pHEAA-AAc-Fe^{3+} DN gels can achieve breaking strength of 960 kPa, fracture strain of 11, elastic modulus of 600 kPa, toughness/stiffness recovery of 75/51.89% (30 min, 80 °C), and some self-healing property. This physical DN hydrogel can adhere on different untreated surfaces (e.g., glasses, aluminum, ceramics, plastics, titanium, wood, and human skin) with high interfacial toughness of 2619−4414 J/m^2. Agar/pHEAA-AAc-Fe^{3+} DN gel can still retain very high interfacial toughness on the glass in water (1354 J/m^2) and urea (811 J/m^2) solutions. Synergetic interactions of ionic association and hydrogen bonding allow to restrain multiple effective chains and disperse the local stress to maintain the network, leading to high mechanical properties and strong surface adhesion. This work could offer some new insights into the design of highly mechanical, self-recoverable, and surface adhesive hydrogels for different significant applications such as wearable devices, soft electronics, and flexible and adhesive supercapacitors.

ASSOCIATED CONTENT

Supporting Information

The Supporting Information is available free of charge at https://pubs.acs.org/doi/10.1021/acsapm.9b00889.

> Preparation conditions and mechanical properties of Agar/pHEAA-AAc-Fe3+ DN gels as a function of network compositions; comparison of energy dissipation between different hydrogels by loading−unloading tests; different solvent-induced swelling effects and mechanical reduction of pHEAA-AAc-Fe3+ DN gels (PDF)

AUTHOR INFORMATION

Corresponding Authors

*E-mail: xlj235@163.com. (L.X.)
*E-mail: zhengj@uakron.edu. (J.Z.)

ORCID

Lijian Xu: 0000-0002-1195-6767
Ting Wang: 0000-0002-7518-6298
Zhang-Qi Feng: 0000-0002-1684-588X
Yung Chang: 0000-0003-1419-4478
Xiong Gong: 0000-0001-6525-3824
Ge Zhang: 0000-0001-8339-1892
Jie Zheng: 0000-0003-1547-3612

Author Contributions

¶These authors contribute equally to this work.

Notes

The authors declare no competing financial interest.

ACKNOWLEDGMENTS

J.Z. is thankful for the financial support from NSF (DMR-1607475 and CMMI-1825122).

REFERENCES

(1) Zhang, D.; Fu, Y.; Huang, L.; Zhang, Y.; Ren, B.; Zhong, M.; Yang, J.; Zheng, J. Integration of antifouling and antibacterial properties in salt-responsive hydrogels with surface regeneration capacity. *J. Mater. Chem. B* **2018**, *6* (6), 950−960.

(2) Zhang, D.; Yao, Y.; Wu, J.; Protsak, I.; Lu, W.; He, X.; Xiao, S.; Zhong, M.; Chen, T.; Yang, J. Super Hydrophilic Semi-IPN Fluorescent Poly(N-(2-hydroxyethyl)acrylamide) Hydrogel for Ultrafast, Selective, and Long-Term Effective Mercury(II) Detection in a Bacteria-Laden System. *ACS Applied Bio Materials* **2019**, *2* (2), 906−915.

(3) Lu, W.; Ma, C.; Zhang, D.; Le, X.; Zhang, J.; Huang, Y.; Huang, C.-F.; Chen, T. Real-Time in Situ Investigation of Supramolecular Shape Memory Process by Fluorescence Switching. *J. Phys. Chem. C* **2018**, *122* (17), 9499−9506.

(4) He, X.; Zhang, D.; Wu, J.; Wang, Y.; Chen, F.; Fan, P.; Zhong, M.; Xiao, S.; Yang, J. One-pot and One-step Fabrication of Salt-responsive Bilayer Hydrogels with 2D and 3D Shape Transformations. *ACS Appl. Mater. Interfaces* **2019**, *11* (28), 25417−25426.

(5) Li, P.; Zhang, D.; Zhang, Y.; Lu, W.; Zhang, J.; Wang, W.; He, Q.; Théato, P.; Chen, T. Aggregation-Caused Quenching-Type Naphthalimide Fluorophores Grafted and Ionized in a 3D Polymeric Hydrogel Network for Highly Fluorescent and Locally Tunable Emission. *ACS Macro Lett.* **2019**, *8*, 937−942.

(6) Dong, L.; Agarwal, A. K.; Beebe, D. J.; Jiang, H. Adaptive liquid microlenses activated by stimuli-responsive hydrogels. *Nature* **2006**, *442* (7102), 551−4.

(7) Kopecek, J. Hydrogels from Soft Contact Lenses and Implants to Self-Assembled Nanomaterials. *J. Polym. Sci., Part A: Polym. Chem.* **2009**, *47* (22), 5929−5946.

(8) Parente, M. E.; Ochoa Andrade, A.; Ares, G.; Russo, F.; Jimenez-Kairuz, A. Bioadhesive hydrogels for cosmetic applications. *Int. J. Cosmet. Sci.* **2015**, *37* (5), 511−8.

(9) Drury, J. L.; Mooney, D. J. Hydrogels for tissue engineering: scaffold design variables and applications. *Biomaterials* **2003**, *24* (24), 4337−4351.

(10) Hoare, T. R.; Kohane, D. S. Hydrogels in drug delivery: Progress and challenges. *Polymer* **2008**, *49* (8), 1993−2007.

(11) Balakrishnan, B.; Mohanty, M.; Umashankar, P. R.; Jayakrishnan, A. Evaluation of an in situ forming hydrogel wound dressing based on oxidized alginate and gelatin. *Biomaterials* **2005**, *26* (32), 6335−42.

(12) Nakajima, T.; Fukuda, Y.; Kurokawa, T.; Sakai, T.; Chung, U.-i.; Gong, J. P. Synthesis and Fracture Process Analysis of Double Network Hydrogels with a Well-Defined First Network. *ACS Macro Lett.* **2013**, *2* (6), 518−521.

(13) Fukao, K.; Nonoyama, T.; Kiyama, R.; Furusawa, K.; Kurokawa, T.; Nakajima, T.; Gong, J. P. Anisotropic Growth of Hydroxyapatite in Stretched Double Network Hydrogel. *ACS Nano* **2017**, *11* (12), 12103−12110.

(14) Gong, J. P. Materials both Tough and Soft. *Science* **2014**, *344* (6180), 161−162.

(15) Gao, G.; Du, G.; Sun, Y.; Fu, J. Self-healable, tough, and ultrastretchable nanocomposite hydrogels based on reversible polyacrylamide/montmorillonite adsorption. *ACS Appl. Mater. Interfaces* **2015**, *7* (8), 5029−37.

(16) Shi, F.-K.; Zhong, M.; Zhang, L.-Q.; Liu, X.-Y.; Xie, X.-M. Robust and self-healable nanocomposite physical hydrogel facilitated by the synergy of ternary crosslinking points in a single network. *J. Mater. Chem. B* **2016**, *4* (37), 6221−6227.

(17) Shao, C.; Chang, H.; Wang, M.; Xu, F.; Yang, J. High-Strength, Tough, and Self-Healing Nanocomposite Physical Hydrogels Based on the Synergistic Effects of Dynamic Hydrogen Bond and Dual Coordination Bonds. *ACS Appl. Mater. Interfaces* **2017**, *9* (34), 28305−28318.

(18) Mayumi, K.; Tezuka, M.; Bando, A.; Ito, K. Mechanics of slide-ring gels: novel entropic elasticity of a topological network formed by ring and string. *Soft Matter* **2012**, *8* (31), 8179.

(19) Murakami, T.; Schmidt, B. V. K. J.; Brown, H. R.; Hawker, C. J. One-Pot "Click" Fabrication of Slide-Ring Gels. *Macromolecules* **2015**, *48* (21), 7774−7781.

DOI: 10.1021/acsapm.9b00889
ACS Appl. Polym. Mater. 2020, 2, 1031−1042

(20) Huang, T.; Xu, H. G.; Jiao, K. X.; Zhu, L. P.; Brown, H. R.; Wang, H. L. A novel hydrogel with high mechanical strength: a macromolecular microsphere composite hydrogel. *Adv. Mater.* **2007**, *19* (12), 1622−1626.
(21) Akimoto, A. M.; Hasuike, E.; Tada, H.; Nagase, K.; Okano, T.; Kanazawa, H.; Yoshida, R. Design of Tetra-arm PEG-crosslinked Thermoresponsive Hydrogel for 3D Cell Culture. *Anal. Sci.* **2016**, *32* (11), 1203−1205.
(22) Matsunaga, T.; Sakai, T.; Akagi, Y.; Chung, U.-i.; Shibayama, M. SANS and SLS Studies on Tetra-Arm PEG Gels in As-Prepared and Swollen States. *Macromolecules* **2009**, *42* (16), 6245−6252.
(23) Chen, H.; Yang, F.; Chen, Q.; Zheng, J. A Novel Design of Multi-Mechanoresponsive and Mechanically Strong Hydrogels. *Adv. Mater.* **2017**, *29* (21), 1606900.
(24) Zhang, Y.; Ren, B.; Yang, F.; Cai, Y.; Chen, H.; Wang, T.; Feng, Z.; Tang, J.; Xu, J.; Zheng, J. Micellar-incorporated hydrogels with highly tough, mechanoresponsive, and self-recovery properties for strain-induced color sensors. *J. Mater. Chem. C* **2018**, *6*, 11536−11551.
(25) Yang, F.; Ren, B.; Cai, Y.; Tang, J.; Li, D.; Wang, T.; Feng, Z.; Chang, Y.; Xu, L.; Zheng, J. Mechanically tough and recoverable hydrogels via dual physical crosslinkings. *J. Polym. Sci., Part B: Polym. Phys.* **2018**, *56*, 1294−1305.
(26) Wu, J.; Han, S.; Yang, T.; Li, Z.; Wu, Z.; Gui, X.; Tao, K.; Miao, J.; Norford, L. K.; Liu, C.; Huo, F. Highly Stretchable and Transparent Thermistor Based on Self-Healing Double Network Hydrogel. *ACS Appl. Mater. Interfaces* **2018**, *10* (22), 19097−19105.
(27) Zhao, S.; Tseng, P.; Grasman, J.; Wang, Y.; Li, W.; Napier, B.; Yavuz, B.; Chen, Y.; Howell, L.; Rincon, J.; Omenetto, F. G.; Kaplan, D. L. Programmable Hydrogel Ionic Circuits for Biologically Matched Electronic Interfaces. *Adv. Mater.* **2018**, *30* (25), 1800598.
(28) Lin, S.; Yuk, H.; Zhang, T.; Parada, G. A.; Koo, H.; Yu, C.; Zhao, X. Stretchable Hydrogel Electronics and Devices. *Adv. Mater.* **2016**, *28* (22), 4497−505.
(29) Kim, S. H.; Jung, S.; Yoon, I. S.; Lee, C.; Oh, Y.; Hong, J. M. Ultrastretchable Conductor Fabricated on Skin-Like Hydrogel-Elastomer Hybrid Substrates for Skin Electronics. *Adv. Mater.* **2018**, *30* (26), 1800109.
(30) Han, L.; Lu, X.; Liu, K.; Wang, K.; Fang, L.; Weng, L.-T.; Zhang, H.; Tang, Y.; Ren, F.; Zhao, C.; Sun, G.; Liang, R.; Li, Z. Mussel-inspired adhesive and tough hydrogel based on nanoclay confined dopamine polymerization. *ACS Nano* **2017**, *11* (3), 2561−2574.
(31) Kurokawa, T.; Furukawa, H.; Wang, W.; Tanaka, Y.; Gong, J. P. Formation of a strong hydrogel-porous solid interface via the double-network principle. *Acta Biomater.* **2010**, *6* (4), 1353−1359.
(32) Yuk, H.; Zhang, T.; Lin, S.; Parada, G. A.; Zhao, X. Tough bonding of hydrogels to diverse non-porous surfaces. *Nat. Mater.* **2016**, *15* (2), 190−6.
(33) Wirthl, D.; Pichler, R.; Drack, M.; Kettlguber, G.; Moser, R.; Gerstmayr, R.; Hartmann, F.; Bradt, E.; Kaltseis, R.; Siket, C. M.; Schausberger, S. E.; Hild, S.; Bauer, S.; Kaltenbrunner, M. Instant tough bonding of hydrogels for soft machines and electronics. *Sci. Adv.* **2017**, *3* (6), 1700053.
(34) Steck, J.; Yang, J.; Suo, Z. Covalent Topological Adhesion. *ACS Macro Lett.* **2019**, *8* (6), 754−758.
(35) Yang, J.; Bai, R.; Li, J.; Yang, C.; Yao, X.; Liu, Q.; Vlassak, J. J.; Mooney, D. J.; Suo, Z. Design molecular topology for wet-dry adhesion. *ACS Appl. Mater. Interfaces* **2019**, *11* (27), 24802−24811.
(36) Niu, R.; Qin, Z.; Ji, F.; Xu, M.; Tian, X.; Li, J.; Yao, F. Hybrid pectin-Fe(3+)/polyacrylamide double network hydrogels with excellent strength, high stiffness, superior toughness and notch-insensitivity. *Soft Matter* **2017**, *13* (48), 9237−9245.
(37) Chen, Q.; Yan, X.; Zhu, L.; Chen, H.; Jiang, B.; Wei, D.; Huang, L.; Yang, J.; Liu, B.; Zheng, J. Improvement of Mechanical Strength and Fatigue Resistance of Double Network Hydrogels by Ionic Coordination Interactions. *Chem. Mater.* **2016**, *28* (16), 5710−5720.
(38) Li, X.; Zhao, Y.; Li, D.; Zhang, G.; Long, S.; Wang, H. Hybrid dual crosslinked polyacrylic acid hydrogels with ultrahigh mechanical strength, toughness and self-healing properties via soaking salt solution. *Polymer* **2017**, *121*, 55−63.
(39) Sun, J. Y.; Zhao, X.; Illeperuma, W. R.; Chaudhuri, O.; Oh, K. H.; Mooney, D. J.; Vlassak, J. J.; Suo, Z. Highly stretchable and tough hydrogels. *Nature* **2012**, *489* (7414), 133−6.
(40) Deng, Y.; Huang, M.; Sun, D.; Hou, Y.; Li, Y.; Dong, T.; Wang, X.; Zhang, L.; Yang, W. Dual Physically Cross-Linked kappa-Carrageenan-Based Double Network Hydrogels with Superior Self-Healing Performance for Biomedical Application. *ACS Appl. Mater. Interfaces* **2018**, *10*, 37544−37554.
(41) Wang, X.-H.; Song, F.; Qian, D.; He, Y.-D.; Nie, W.-C.; Wang, X.-L.; Wang, Y.-Z. Strong and tough fully physically crosslinked double network hydrogels with tunable mechanics and high self-healing performance. *Chem. Eng. J.* **2018**, *349*, 588−594.
(42) Liu, S.; Oderinde, O.; Hussain, I.; Yao, F.; Fu, G. Dual ionic cross-linked double network hydrogel with self-healing, conductive, and force sensitive properties. *Polymer* **2018**, *144*, 111−120.
(43) Chen, Q.; Zhu, L.; Chen, H.; Yan, H. L.; Huang, L. N.; Yang, J.; Zheng, J. A Novel Design Strategy for Fully Physically Linked Double Network Hydrogels with Tough, Fatigue Resistant, and Self-Healing Properties. *Adv. Funct. Mater.* **2015**, *25* (10), 1598−1607.
(44) Chen, H.; Liu, Y.; Ren, B.; Zhang, Y.; Ma, J.; Xu, L.; Chen, Q.; Zheng, J. Super Bulk and Interfacial Toughness of Physically Crosslinked Double-Network Hydrogels. *Adv. Funct. Mater.* **2017**, *27* (44), 1703086.
(45) Chen, F.; Chen, Q.; Zhu, L.; Tang, Z.; Li, Q.; Qin, G.; Yang, J.; Zhang, Y.; Ren, B.; Zheng, J. General strategy to fabricate strong and tough low-molecular-weight gelator-based supramolecular hydrogels with double network structure. *Chem. Mater.* **2018**, *30* (5), 1743−1754.
(46) Henderson, K. J.; Zhou, T. C.; Otim, K. J.; Shull, K. R. Ionically Cross-Linked Triblock Copolymer Hydrogels with High Strength. *Macromolecules* **2010**, *43* (14), 6193−6201.
(47) Roma-Luciow, R.; Sarraf, L.; Morcellet, M. Complexes of poly (acrylic acid) with some divalent, trivalent and tetravalent metal ions. *Eur. Polym. J.* **2001**, *37* (9), 1741−1745.
(48) Zheng, S. Y.; Ding, H.; Qian, J.; Yin, J.; Wu, Z. L.; Song, Y.; Zheng, Q. Metal-Coordination Complexes Mediated Physical Hydrogels with High Toughness, Stick-Slip Tearing Behavior, and Good Processability. *Macromolecules* **2016**, *49* (24), 9637−9646.
(49) Liu, X.; Zhang, Q.; Gao, Z.; Hou, R.; Gao, G. Bioinspired Adhesive Hydrogel Driven by Adenine and Thymine. *ACS Appl. Mater. Interfaces* **2017**, *9* (20), 17645−17652.
(50) Han, L.; Lu, X.; Liu, K.; Wang, K.; Fang, L.; Weng, L. T.; Zhang, H.; Tang, Y.; Ren, F.; Zhao, C.; Sun, G.; Liang, R.; Li, Z. Mussel-Inspired Adhesive and Tough Hydrogel Based on Nanoclay Confined Dopamine Polymerization. *ACS Nano* **2017**, *11* (3), 2561−2574.

DOI: 10.1021/acsapm.9b00889
ACS Appl. Polym. Mater. 2020, 2, 1031−1042